Electronic Supplementary Material (ESI) for New Journal of Chemistry.

# Supplementary Information

## Novel Ag Deposited Nano Coordination Polymers Derived Porous $SnO_2$/NiO Heteronanostructure for Enhanced Photocatalytic Reduction of Cr (VI) under Visible Light

***Md.Rakibuddin and Rajakumar Ananthakrishnan****

*Department of Chemistry, Green Environmental Materials and Analytical Chemistry*

*Laboratory, Indian Institute of Technology, Kharagpur 721 302, India.*

### Instrumentation

Transmission Electron Microscopy (TEM) and High Resolution TEM (HRTEM) were performed with JEOL JEM2010 electron microscope operating at 200 kV. Thermogravimetric Analysis (TGA) was analysed on Perkin-Elmer instrument, Pyris Diamond TG/DTA with $Al_2O_3$ crucible. Powdered X-ray Diffraction (PXRD) has been carried out by Bruker APEX-2 diffractometer. The X-ray Photoelectron Spectroscopy (XPS) was measured by Specs (German). Fourier Transform Infra Red spectra (FT-IR) were carried out with a Perkin-Elmer FT-IR spectrophotometer RXI. Energy Dispersive X-ray (EDX) was measured with FEI TECNAI-G2-20S-TWIN (USA). Photoluminescence (PL) spectra were recorded by F-7000 FL Spectrophotometer. BET surface area and $N_2$ sorption isotherms (77K) were measured by Quantachrome Autosorb-1 instrument. FESEM image and elemental mapping were done with Supra Carl Zeiss 40 instrument.

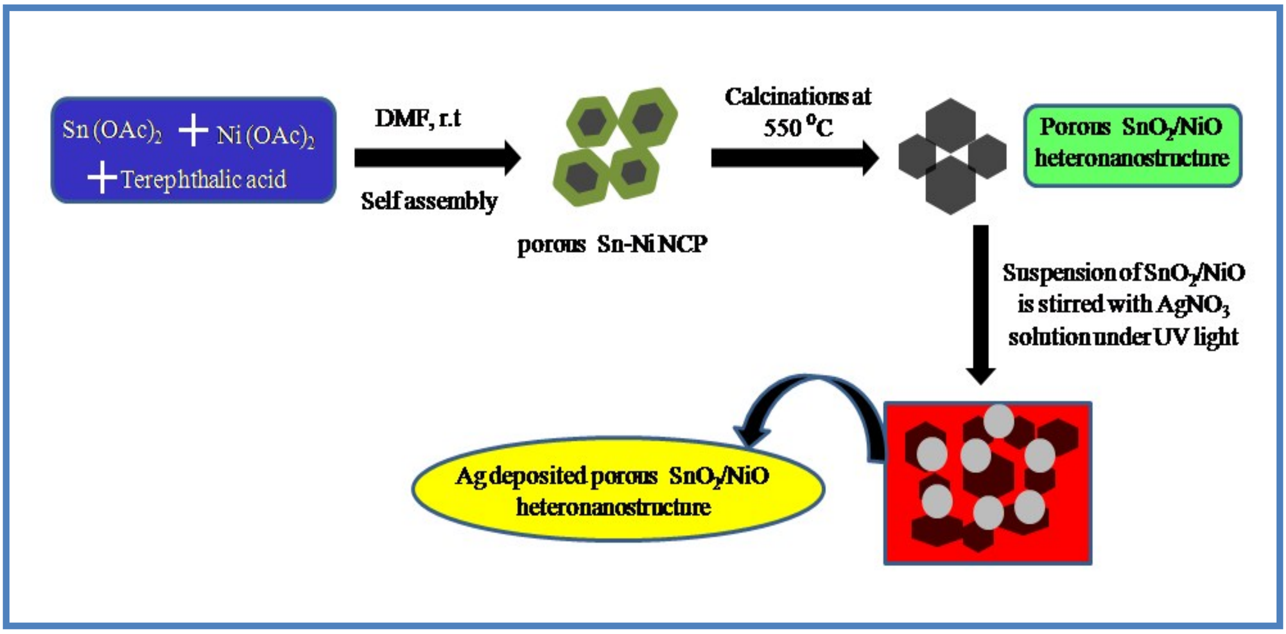

**Scheme 1** Schematic representation for the formation of Ag/$SnO_2$/NiO heteronanostructure from the NCP precursor.

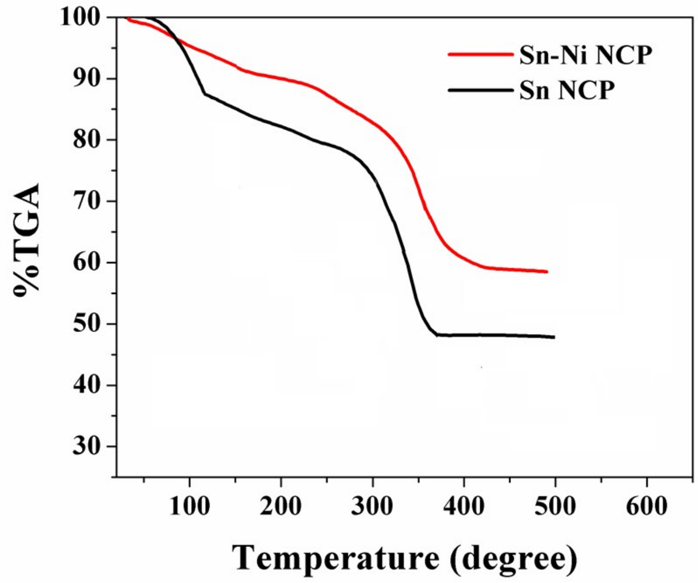

Figure S1: TGA analysis of the Sn NCP and Sn-Ni NCP under $N_2$ atmosphere at the heating rate 10° C /min.

TGA shows a minor weight loss at around 125-175 °C due to loss of water molecules from the NCPs, and a major weight losses at around 300 °C and 350 °C due to presence of terephthalate organic ligands in the NCPs. It also informs that thermal stability of the mixed-metal Sn-Ni NCP (~40 % weight loss) is greater than single metal NCP (~55% weight loss).

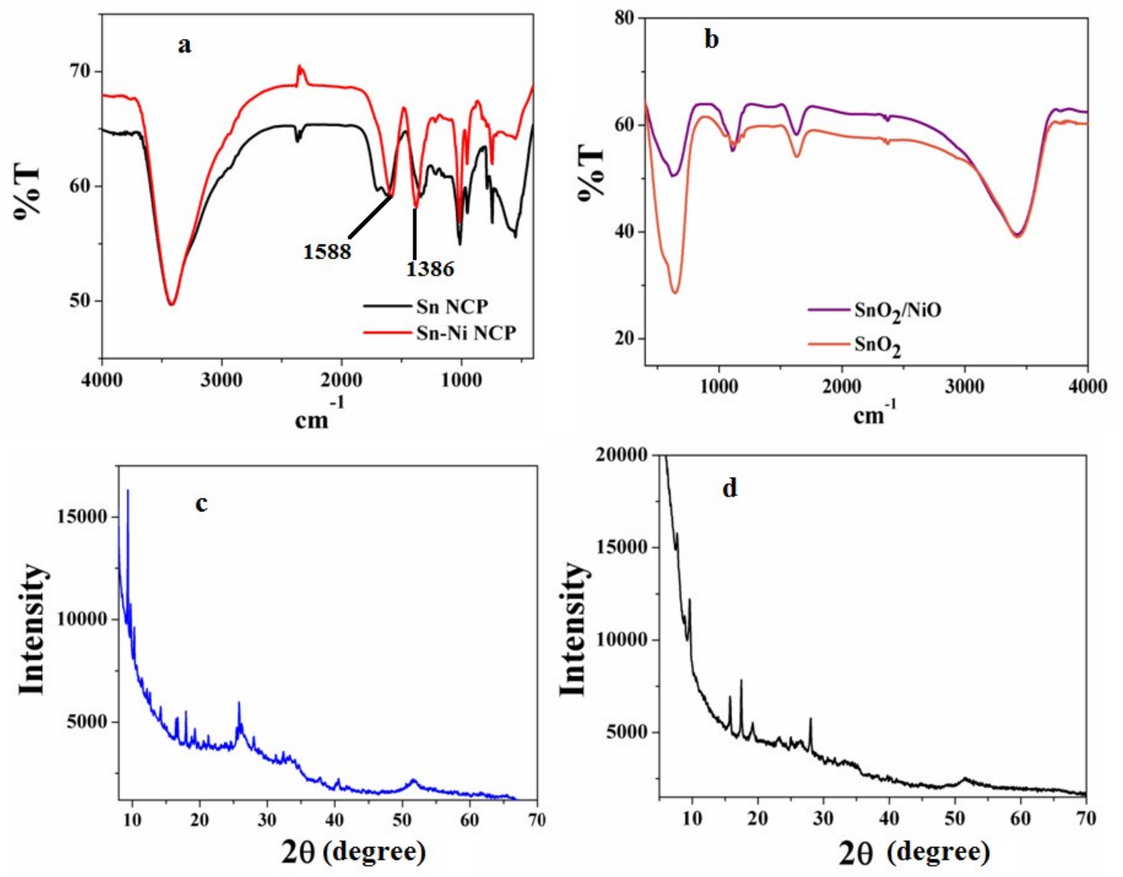

Figure S2: FT-IR analysis of the a) Sn NCP and Sn-Ni NCP, b) $SnO_2$ and $SnO_2$-NiO obtained from corresponding Sn-NCP and Sn-Ni NCP after calcinations at 450 ºC; c) PXRD pattern of the Sn-Ni NCP and d) PXRD of the Sn-NCP.

The CO stretching frequency shifted to 1588 $cm^{-1}$ from 1686 $cm^{-1}$ for the un-coordinated ligand 1,4-$H_2BDC$ after the formation of coordination polymers with $Sn^{2+}/Ni^{+2}$ ions.[1] A strong and broad peak at around 3384 $cm^{-1}$ is observed typical for $H_2O$ molecules with hydrogen bonds, indicating that $H_2O$ molecules participate in the coordination of $Sn^{+2}/Ni^{+2}$ in the NCP structures. The peak at 1386 $cm^{-1}$ in the Sn-Ni NCPs is due to carboxylate stretching frequencies of the ligand, $BDC^{2-}$.[2] Interestingly, all the aromatic peaks are vanished after calcinations of the NCPs at 450 $^0$C for 90 min suggesting the formation of metal oxide hetero-nanostructures.

The PXRD of the NCPs reveals sharp peaks, and hence, indicates crystalline nature of the NCPs (c-d). The PXRD pattern also indicates that the two NCP materials are not iso-structural.

1. S. Jung, W.Cho, H. J.Lee and M. Oh, *Angew. Chem. Int. Ed*. 2009, **48**, 1459-1462.
2. M. Rakibuddin and R. Ananthakrishnan, *RSC Adv*. 2015, **5**, 68117.

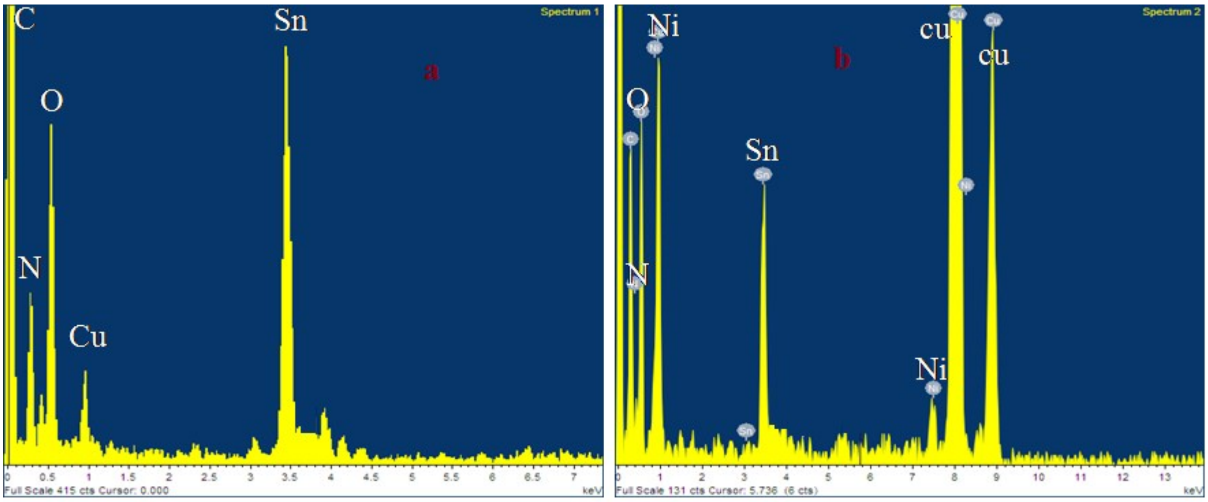

Figure S3: EDX elemental analysis of the a) Sn NCP and b) Sn-Ni NCP.

EDX shows the presence of C, N, O, Sn and Ni in the NCP structures. The presence of Cu is due to Cu grid used during TEM sample preparation.

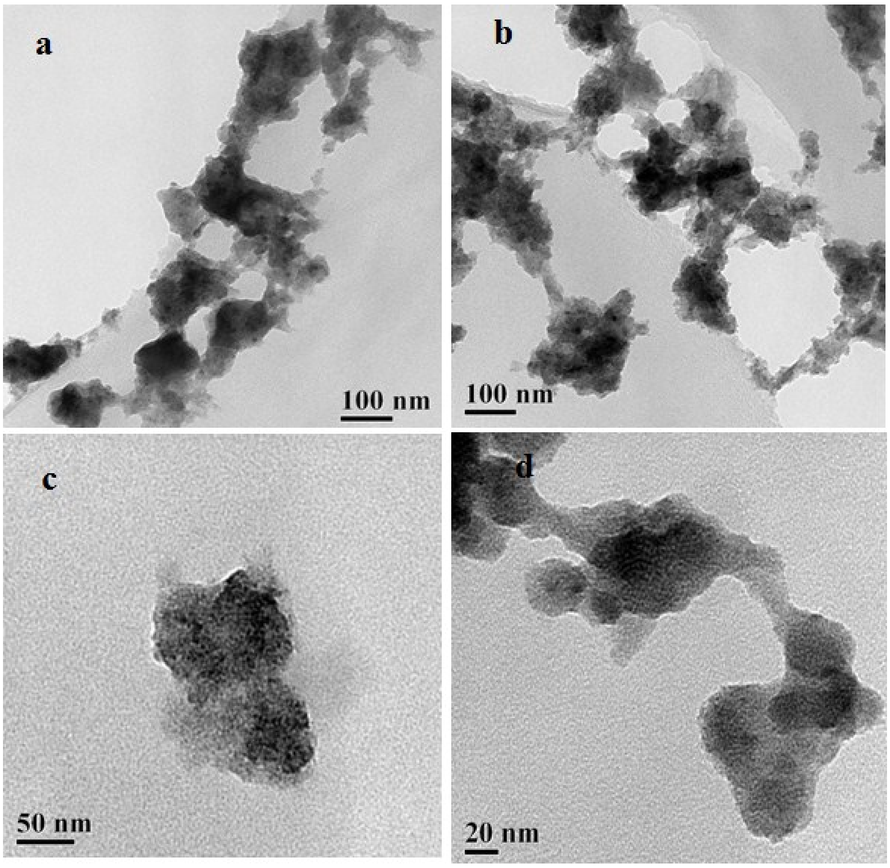

FigureS4. TEM image of the porous a-b) Sn NCP and c-d) Sn-Ni mixed metal NCP.

TEM image of the Sn NCP and Sn-Ni NCPs reveals the formation of aggregated lump type porous particles.

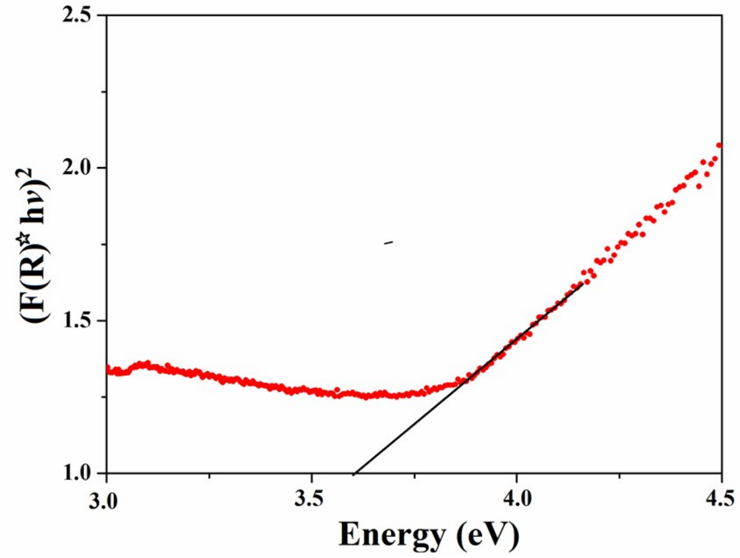

Figure S5. Plot of [F(R) hν]$^2$ versus photon energy (hν) for determination of band gap of the as-synthesized pure $SnO_2$.

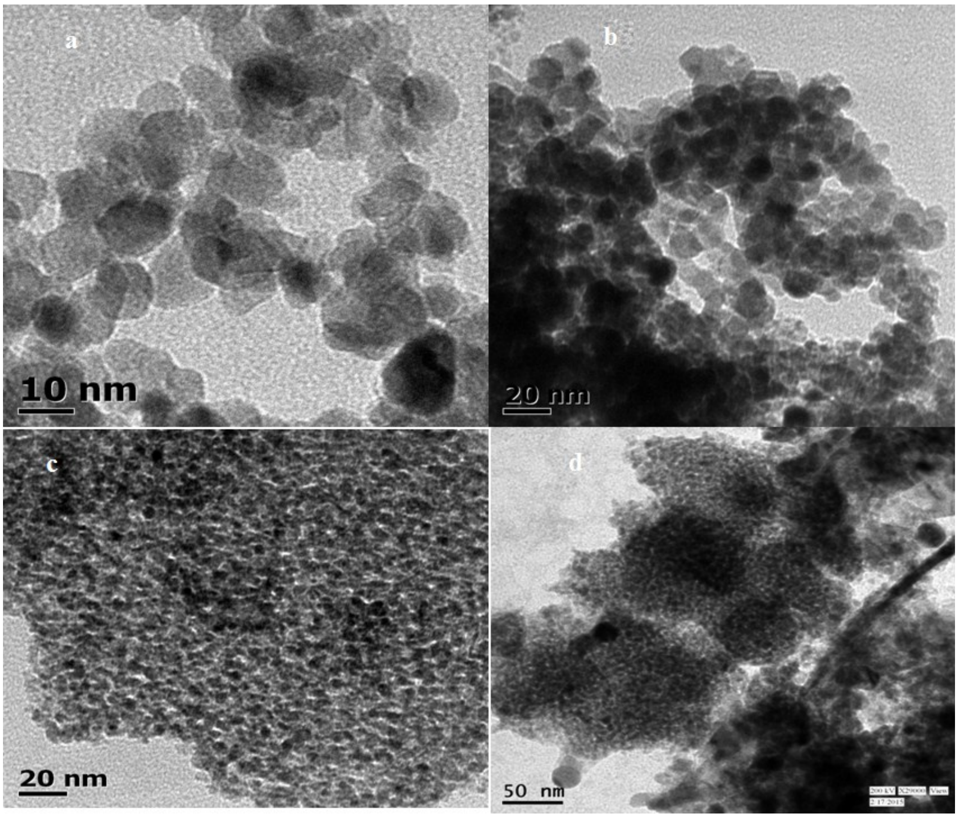

FigureS6. TEM image of the a) SnO$_2$, b) SnO$_2$/NiO, c) only NiO in the SnO$_2$/NiO and d) Ag/Sn-SnO$_2$/NiO obtained after calcinations of the corresponding NCPs.

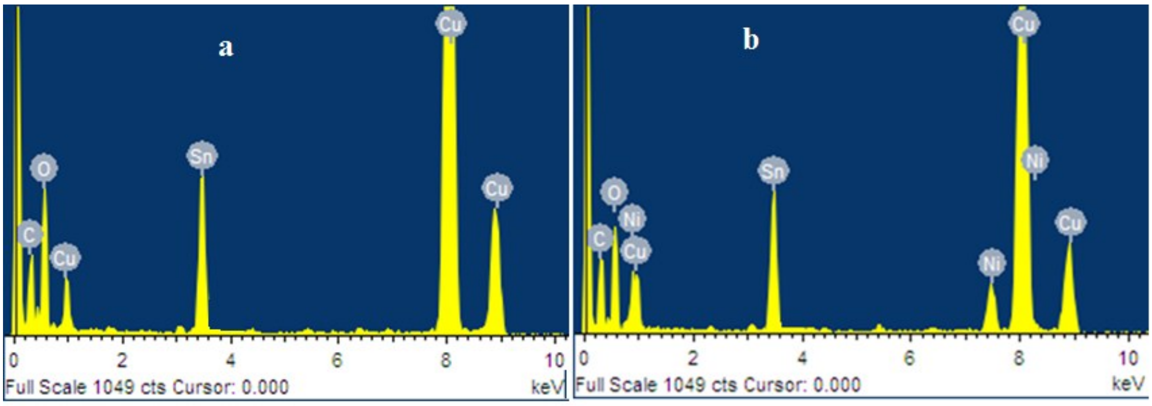

Figure S7. Energy dispersive X-ray analysis of the a) $SnO_2$ and b) $SnO_2$/NiO heteronanostructure.

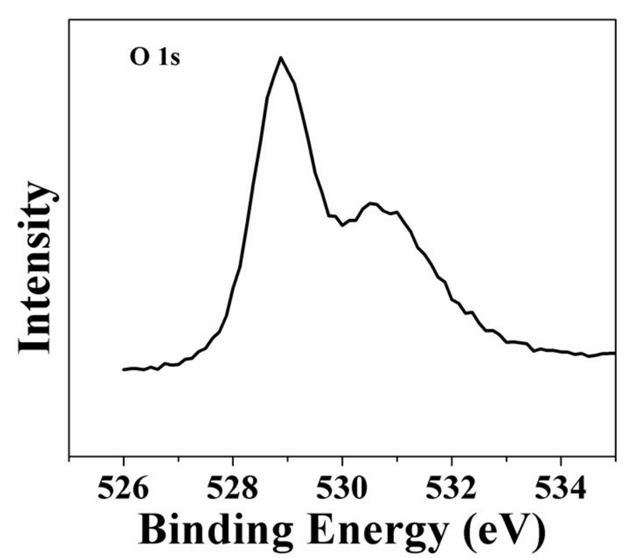

FigureS8. High resolution XPS of the O 1s in the Ag/$SnO_2$/NiO heteronanostructure.

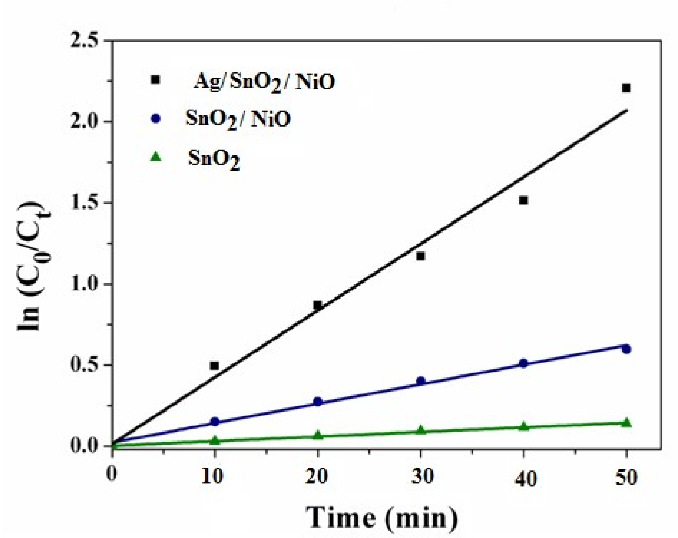

Figure S9. ln $C_0/C_t$ vs Time plot for the reduction of Cr (VI) in presence of the different catalyst under visible light.

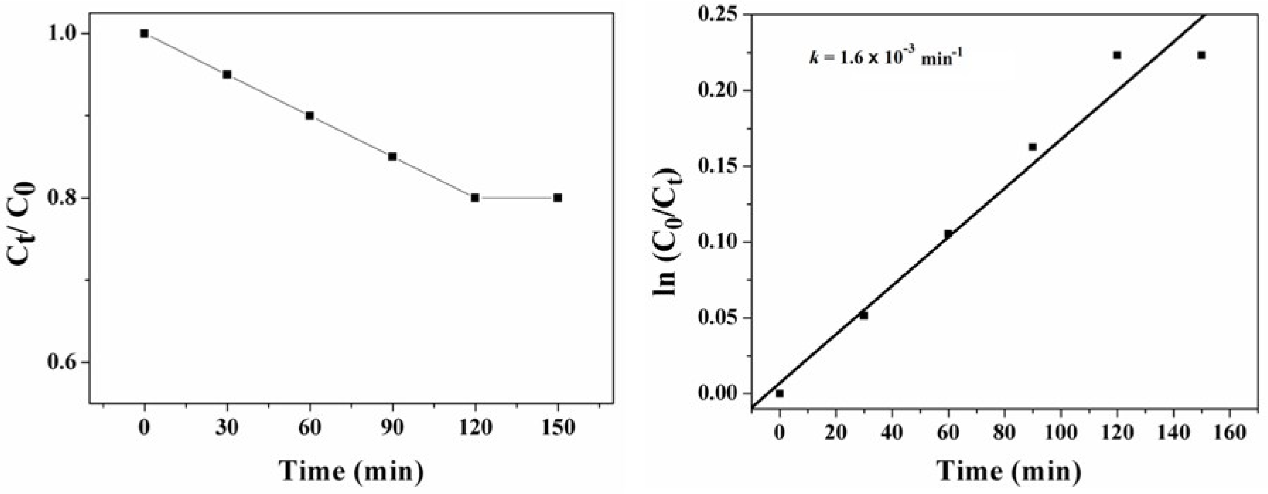

Figure S10. a) Dark adsorption Kinetic plots ($C_t/C_0$ vs Time) and b) ln $C_0/C_t$ vs Time plot of Cr(VI) solution in the presence of Ag/$SnO_2$/NiO .

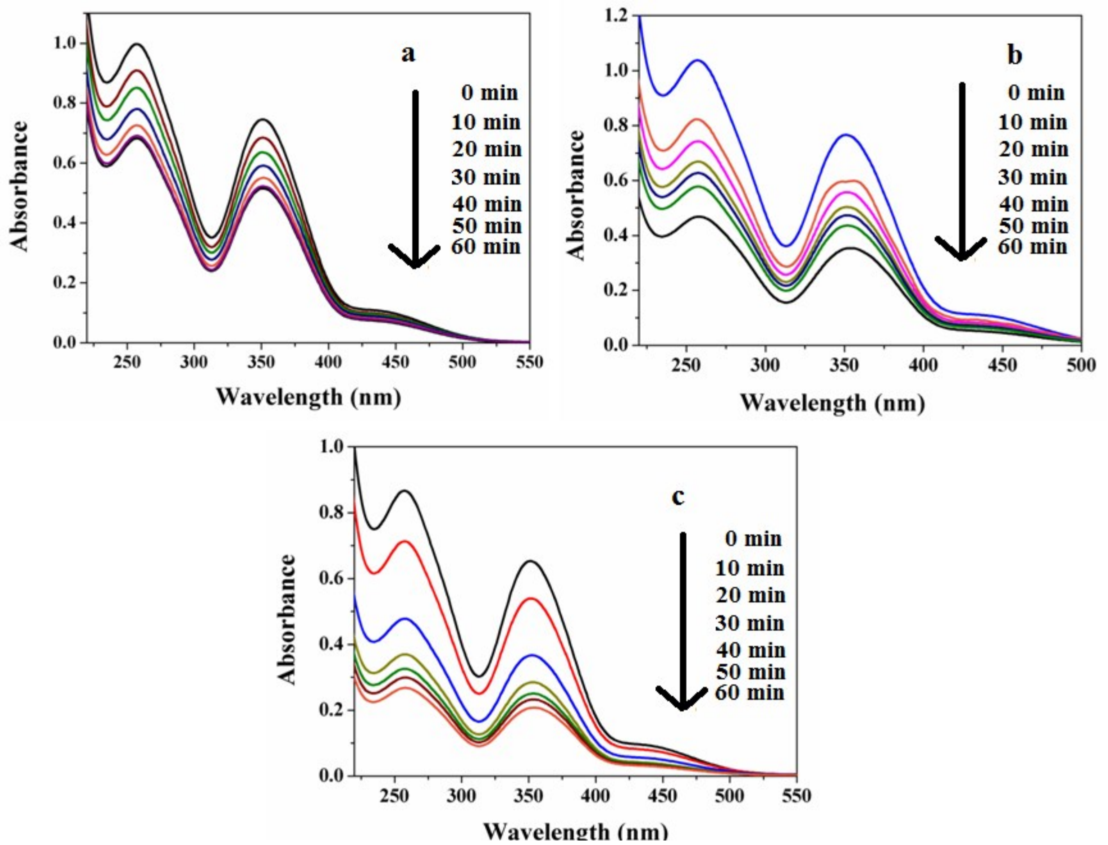

Figure S11. UV-Visible absorption spectra for reduction of Cr(VI) at the catalyst dose a) 0.25 g/L, b) 0.5 g/L and c) 0.75 g/L of the Ag/$SnO_2$/NiO catalyst [Cr(VI)]=20 mg/L, pH=2.0].

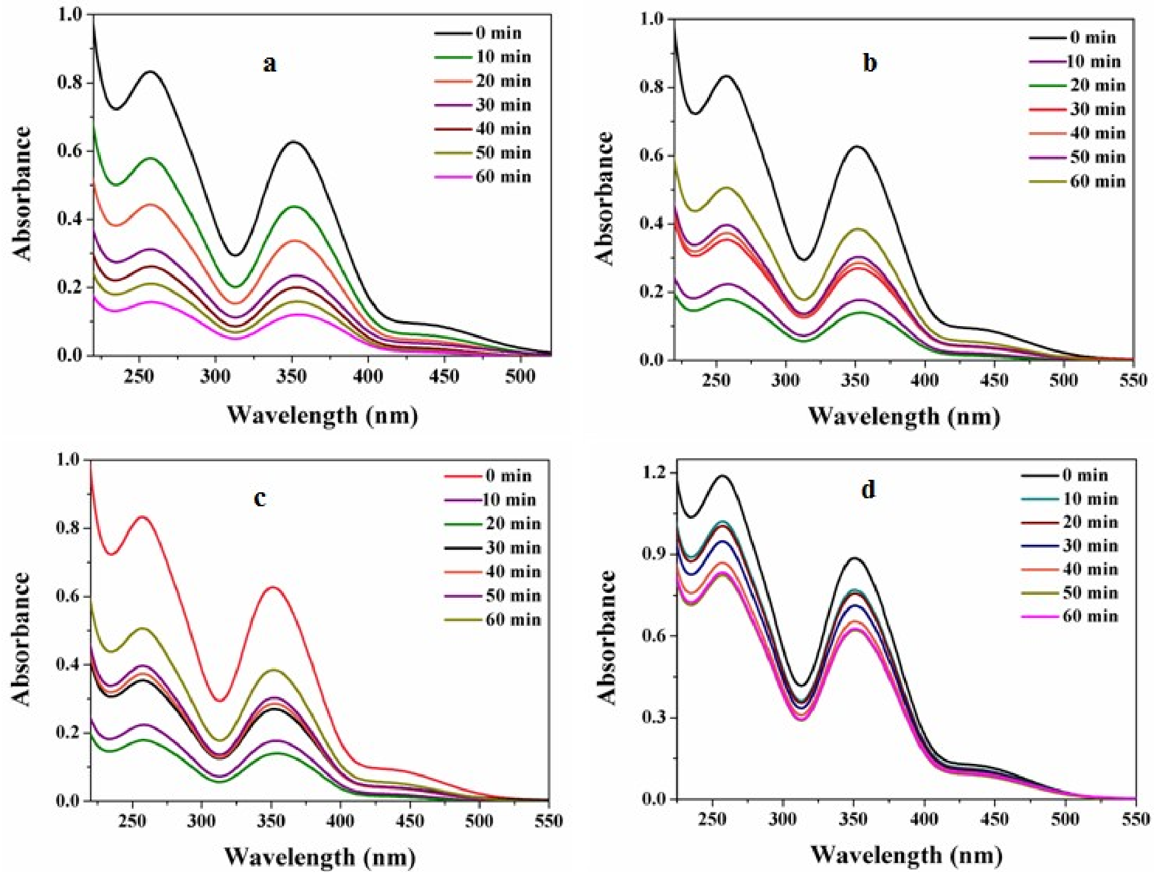

Figure S12. UV-Visible absorption spectra for reduction of Cr(VI) at different pH a) pH 4.0, b) pH 6.0 c) 8.0 and d) pH 10.0 in presence of the Ag/$SnO_2$/NiO catalyst [Cr(VI)]=20 mg/L, [catalyst]= 1.0 g/L].

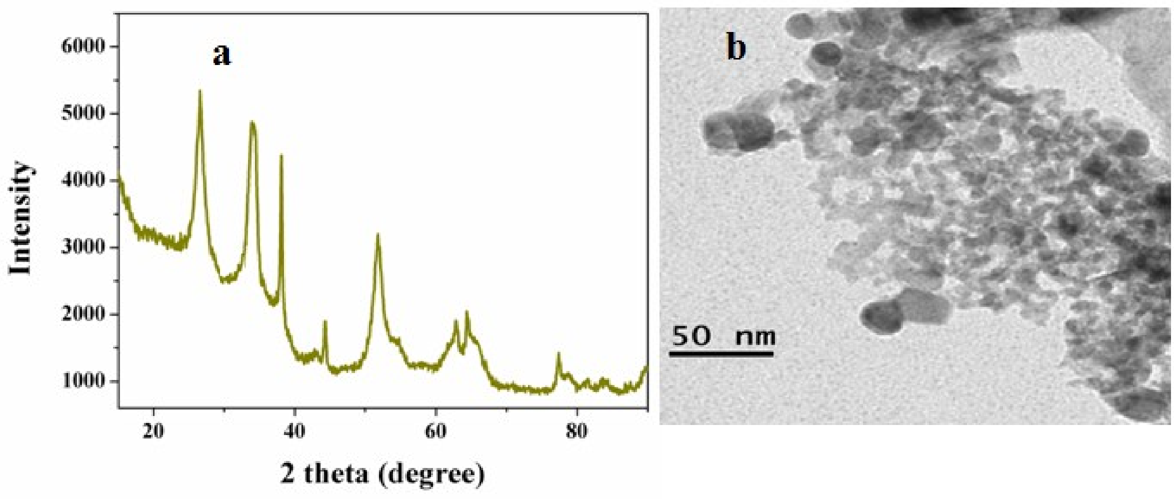

Figure S13. a) PXRD pattern of the reused catalyst (after 5th cycle) after photo-reduction of Cr(VI) and b) TEM image of the Ag/$SnO_2$/NiO catalyst after 5th cycle of the photoreduction.

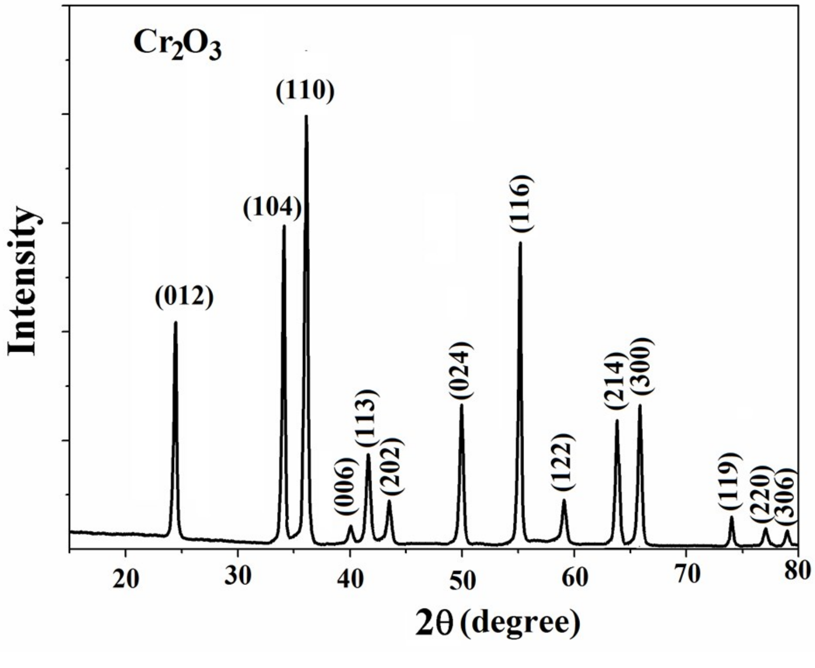

Figure S14. PXRD pattern of the sediment after heating at 400 ºC for 1 h.